Influences of the Hydrophobicity of the Heme-binding Pocket on the Properties and Functions of Cytochrome b_5 *Mutants*

GAN, Jian-Hua[a] (甘建华) **WANG, Yun-Hua**[b] (王韵华) **WU, Jian**[#,a] (邬键)
HUANG, Zhong-Xian[*,b] (黄仲贤) **XIA, Zong-Xiang**[*,a] (夏宗芗)
[a] *State Key Laboratory of Bioorganic and Natural Products Chemistry, Shanghai Institute of Organic Chemistry, Chinese Academy of Sciences, Shanghai 200032, China*
[b] *Chemical Biology Laboratory, Department of Chemistry, Fudan University, Shanghai 200433, China*

The mutation sites of the four mutants F35Y, P40V, V45E and V45Y of cytochrome b_5 are located at the edge of the heme-binding pocket. The solvent accessible areas of the "pocket interior" of the four mutants and the wild-type cytochrome b_5 have been calculated based on their crystal structures at high resolution. The change in the hydrophobicity of the heme-binding pocket resulting from the mutation can be quantitatively described using the difference of the solvent accessible area of the "pocket interior" of each mutant from that of the wild-type cytochrome b_5. The influences of the hydrophobicity of the heme-binding pocket on the protein stability and redox potential are discussed.

Keywords cytochrome b_5, mutant, heme-binding pocket, solvent accessible area, hydrophobicity, structure-function relationship

Introduction

Electron transfer reactions are the key steps in photosynthesis, respiration and many other biochemical processes.[1] Cytochrome b_5 is a redox protein existing widely in nature, which acts as an electron-carrier during various electron transfer processes in the biological system.[2]

Cytochrome b_5 is a membrane protein with molecular weight of approximately 16 kDa, of which the hydrophobic C-terminal domain anchors cytochrome b_5 to the membrane, and the hydrophilic N-terminal domain contains heme prosthetic group and exhibits the biological functions of the intact cytochrome b_5.[3]

Proteolyzed by lipase or trypsin, cytochrome b_5 produces a soluble N-terminal fragment. The crystal structure of the former was reported earlier.[4-6] We prepared the recombinant wild-type fragment of the latter which is referred to as WT-Tb_5, and its crystal structure was determined.[7] The heme prosthetic group is bound in a hydrophobic pocket, which is shown in Fig. 1a. Four helices (αII: L32—H39, αIII: E43—A50, αIV: A54—V61, αV: S64—I75) form the wall and three β-strands (βII: T21—L25, βIII: Y27—L32, βIV: G51—A54) form the bottom of the heme-binding pocket, and the top part of the heme is exposed to the aqueous environment.

Site-directed mutagenesis combined with X-ray crystallography, NMR, spectrometry, electrochemistry and kinetics were used to study the structure-function relationship of cytochrome b_5.[8-12]

We prepared seven mutants of Tb_5 and determined their crystal structures as well as the properties and functions.[7,13-19] The seven mutants are grouped into two types according to the locations of the mutation sites: the first type includes F35Y, P40V, V45E, V45Y, V61H,[13-16] with the mutation sites at the edge of the heme-binding pocket, as shown in Fig. 1b; the second type includes E44/56A and a quadruple-site mutant,[17] with the mutation sites at some negatively charged amino acid residues located at the molecular surface, which are involved in the interactions with cytochrome *c* and greatly influence the electron transfer rate. Based on the crystal structures and various properties and functions of WT-Tb_5 and its seven mutants, the relationship between the structures and properties or functions was previously discussed in detail for each mutant respectively, and a variety of influencing factors were suggested.[7,13-17]

In this paper, based on the comprehensive analysis of the structure-function relationship, we focus on the first type of the mutants. For WT-Tb_5 and four of the five mutants of this type, F35Y, P40V, V45E and V45Y, the crystal structures were determined at high resolution (0.18—0.19 nm). The solvent accessible areas of the "pocket interior" of WT-Tb_5 and these four mutants were calculated, and the difference of the area of each mutant from that of WT-Tb_5 was taken as the quantitative description of the hydrophobicity change of the heme-binding pocket resulting from the mutation. The redox potentials and the protein stability of F35Y, P40V, V45E and V45Y are

* E-mail: xiazx@mail.sioc.ac.cn; zxhuang@fudan.edu.cn
# Present address: Department of Chemistry and Biochemistry, University of California at San Diego, San Diego, CA 92093, USA.
Received April 10, 2003; revised and accepted June 20, 2003.
Project supported by the National Natural Science Foundation of China (Nos. 39970159, 29731030, 39990600).

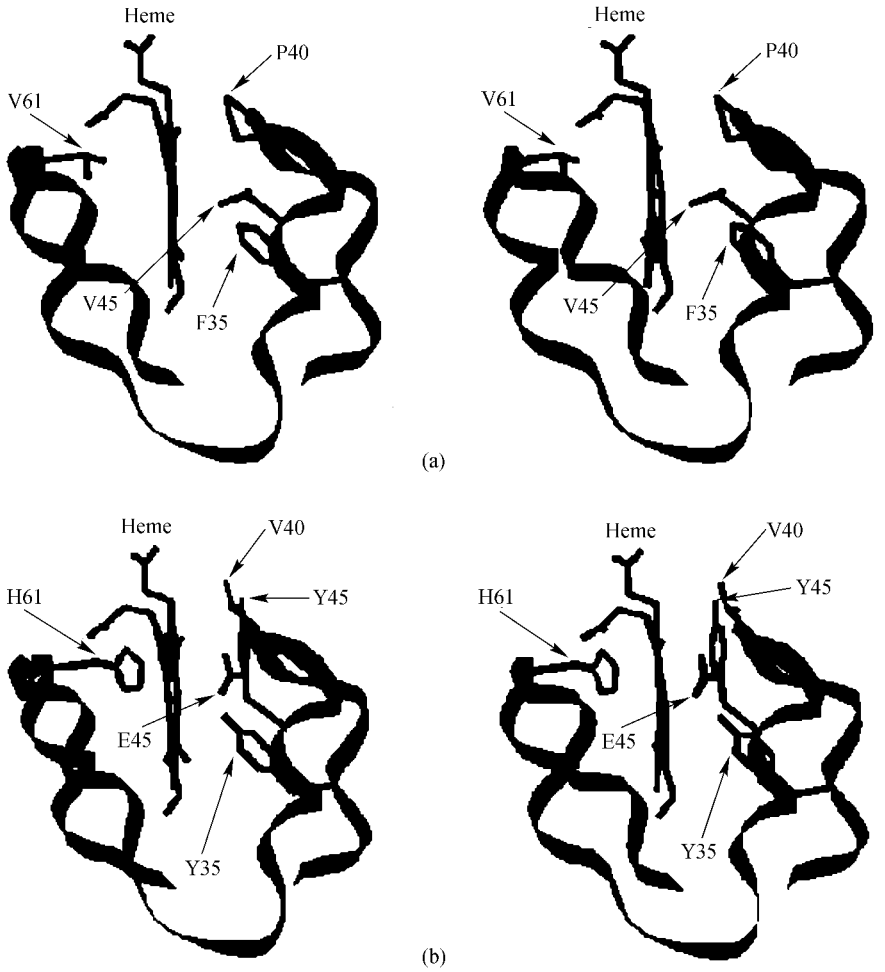

Fig. 1 Stereo ribbon diagrams of the heme-binding pocket of WT-*Tb*$_5$ and the first type of mutants. (a) Heme and the side chains of F35, P40, V45 and V61 in WT-*Tb*$_5$ are shown. (b) Heme and the side chains of Y35, V40, E45, Y45 and H61 in the first type of mutants are superimposed and shown. These diagrams were prepared using the program SETOR.[22]

summarized in Table 1. The influences of the hydrophobicity of the heme-binding pocket on the protein stability and redox potential are discussed. This paper does not deal with one of the first type of mutants, V61H, because its crytsal structure was determined at lower resolution and the calculated solvent accessbility based on its crystal structure could not be compared with that of WT-*Tb*$_5$ with sufficient accuracy.

Table 1 The calculated solvent accessible area of the "pocket interior" of WT-*Tb*$_5$ and the four mutants as well as their redox potentials and stability

	WT-*Tb*$_5$	F35Y	P40V	V45E	V45Y
Resolution of crystal structure (nm)	0.19	0.18	0.19	0.18	0.19
Solvent accessible area (nm^2)	29.90	29.83	30.17	30.16	30.39
Solvent accessible area difference[a] (nm^2)		−0.07	0.27	0.26	0.49
Redox potential shift[b] (mV)		−66	−40	−23	−32
ΔT_m shift[c] (℃)		3.4	−8.6	−9.9	−6.2
$\Delta(\Delta G_D^{50\%})$[d] (kJ/mol)		3.3	−10.0	−11.2	−6.4
ΔC_m shift[e] (mol/L)		1.2	−1.4	−2.0	−1.2
$\Delta(\Delta G_D^{50\%})$[f] (kJ/mol)		4.3	−5.3	−8.0	−4.0

[a] The difference of the solvent accessible area of the "pocket interior" of the mutant from that of WT-*Tb*$_5$. [b] The redox potential shift of the mutants, compared with WT-*Tb*$_5$. [c] The shift of the midpoint temperature of transition of the oxidized mutant, compared with that of WT-*Tb*$_5$. [d] Difference in free energy at the midpoint of denaturation induced by heat, between the mutant and WT-*Tb*$_5$. [e] The shift of the concentration of urea to produce 50% unfolded protein, compared with that of WT-*Tb*$_5$. [f] Difference in free energy at the midpoint of denaturation induced by urea, between the mutant and WT-*Tb*$_5$.

Materials and methods

The procedure to prepare the four mutants and the methods to determine the protein stability and redox potentials were described previously.[14,18,19]

The complete crystal structure of WT-Tb_5[7] is shown in Fig. 2a (left). The upper part of the WT-Tb_5 structure containing the prosthetic group heme can be obtained by removing water molecules and the amino acid residues which are not involved in the wall or bottom of the heme pocket, *i.e.* the 20 N-terminal residues, the 8 C-terminal residues and the segment H26—K28. The inside wall and bottom of the upper part of the WT-Tb_5 structure comprise the hydrophobic heme-binding pocket. However, there are some hydrophilic or charged side chains distributed at its outside surface that are flexible in conformation and point into the solvent in the direction approximately perpendicular to the surface of the pocket, such as W22, D31, K34, E37, E38, E43, E44, R47, E48, D53, E56, D60, T65, D66, E69, K72. These side chains were removed from the outside wall or bottom of the upper part of the structure of the WT-Tb_5. The obtained structure, containing heme group, was referred to as "pocket interior" in this paper, which is shown in Fig. 2a (right) and Fig. 2b, and the solvent accessible area of it was calculated for WT-Tb_5 and each mutant using the program AREAIMOL of the CCP4 suite.[20,21]

Results and discussion

Quantitative description of the hydrophobicity of the heme-binding pocket

The hydrophobicity of the heme-binding pocket could be quantitatively described using the solvent accessible area inside the heme-binding pocket. However, the calcu-

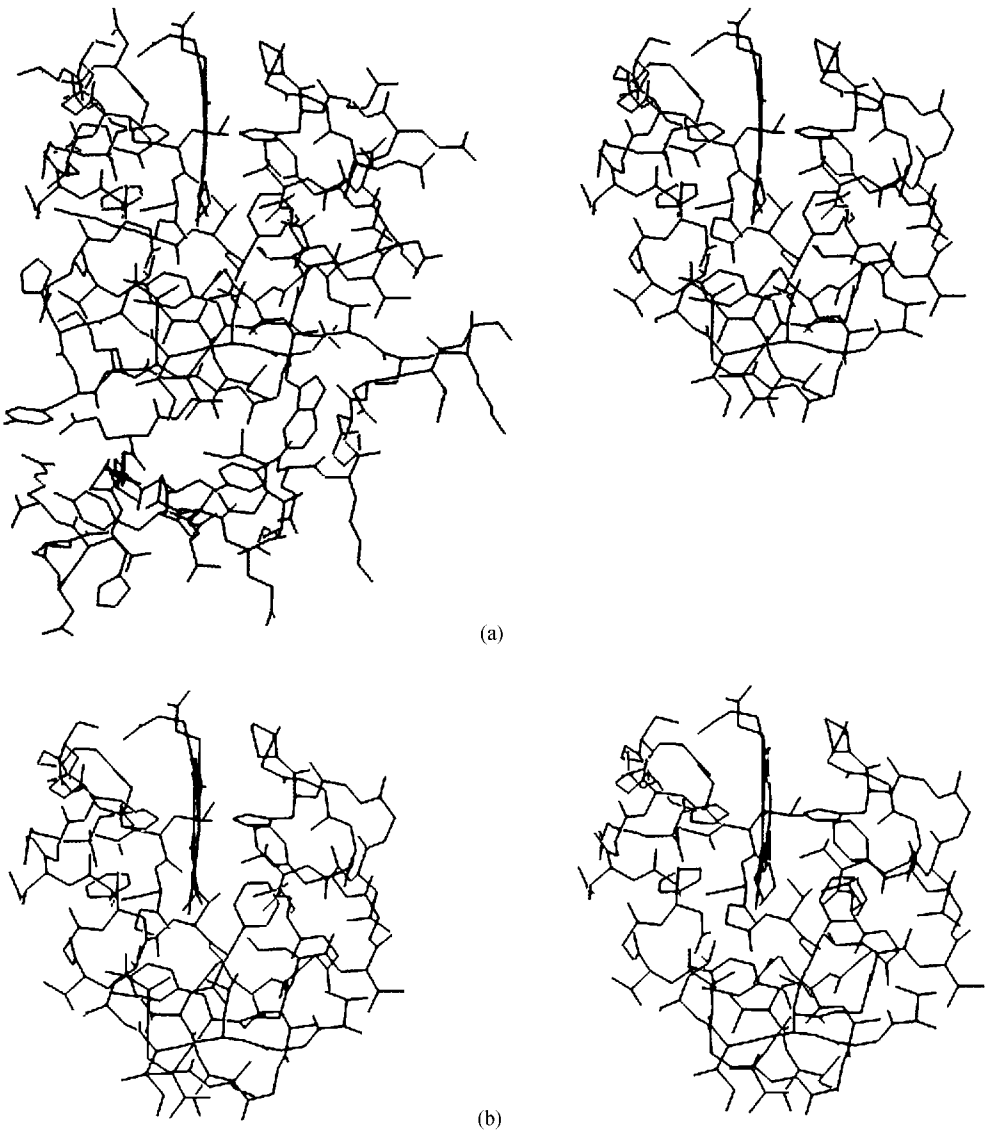

Fig. 2 (a) Left: The complete crystal structure of WT-Tb_5. Water molecules are not shown. Right: The structure of "pocket interior" of WT-Tb_5. (b) The stereo diagram of the "pocket interior" structure of WT-Tb_5. These diagrams were prepared using the program TURBO-FRODO.[23]

lated solvent accessible area of the heme-binding pocket includes not only the interior surface but also the exterior surface of the heme-binding pocket that are solvent accessible. Since "pocket interior" was generated by removing the hydrophilic side chains of the outside surface of the heme-binding pocket, the solvent accessibility of the exterior surface of the "pocket interior" is contributed only by the amino nitrogen and the carbonyl oxygen atoms of the main chain as well as some side chains which constitute a part of the pocket wall. This contribution from each mutant is almost the same as that from WT-Tb_5 because the overall structure does not change due to the mutation and those side chains show conserved conformations in WT-Tb_5 and various mutants.[7,13-17] Therefore, the change in the hydrophobicity of the heme-binding pocket of each mutant relative to WT-Tb_5 could be quantitatively described using the difference of the solvent accessible area of the "pocket interior" of the mutant from that of WT-Tb_5, the more positive the difference, the lower the hydrophobicity.

Solvent accessible areas of the "pocket interior" of WT-Tb_5 and its mutants

The calculation was based on the crystal structures of WT-Tb_5 and its four mutants, refined at 0.18—0.19 nm resolution. Table 1 lists the solvent accessible areas of the "pocket interior" of WT-Tb_5 and the four mutants, F35Y, P40V, V45E and V45Y. Compared with WT-Tb_5, the solvent accessible areas of the "pocket interior" increase by 0.26—0.49 nm^2 for P40V, V45E and V45Y, and it decreases by 0.07 nm^2 for F35Y.

Influence of the hydrophobicity of heme-binding pocket on protein stability

The heme prosthetic group is located in a hydrophobic pocket in the cytochrome b_5. The hydrophobicity of the pocket is necessary to maintain the stability of cytochrome b_5. Cytochrome b_5 denaturates toward heat or denaturants due to the dissociation of the heme from the protein.

In the structure of WT-Tb_5 the side chains of some hydrophobic key residues such as F35, P40 and V45, are located at the edge of the heme-binding pocket, pointing to the heme plane.[4-6,7] They form the "gates" at the edge of the heme-binding pocket (Fig. 1a), preventing the access of solvent into the pocket and maintaining its proper hydrophobicity, which was demonstrated by the crystal structure of WT-Tb_5 in which no solvent molecule was observed in the heme-binding pocket.[7]

In the V45E and V45Y mutants E45 and Y45 are polar or charged residues, and their side chains are too large to be accommodated inside the heme pocket and are forced to point into solvent. In the P40V mutant the side chain of V40 also points into solvent to avoid the unreasonably close contacts although it is a hydrophobic residue. In these mutants the gates at the edge of the heme-binding pocket are thus open and the solvent accessibility of the pocket is increased, as shown in Table 1. Especially in V45Y, the phenol ring of Y45 is almost parallel to the mean plane of heme, and the gate is greatly opened, giving the highest difference of the solvent accessible area of the "pocket interior" (0.49 nm^2). The higher solvent accessibility of these mutants than that of WT-Tb_5 is verified by the fact that water molecules are found in the heme-binding pocket in the P40V and V45Y mutant structures.[14,15] For example, a water molecule is introduced to the entrance of the heme-binding pocket in the V45Y mutant, forming hydrogen bonds to the main chain carbonyl oxygen of Y45 as well as the side chains of E48 and Q49, and this water molecule does not exist in WT-Tb_5. It indicates that the calculated solvent accessible area of the "pocket interior" is supported by the results from X-ray experiments.

In these three mutants, the hydrophobicity of the heme-binding pocket is reduced resulting from the mutation, so that the heme dissociation toward heat or denaturants is easier to take place than in the WT-Tb_5, leading to the less stability of these mutants than the wild-type protein, which is shown in Table 1.

The structure of F35Y mutant obviously differs from the above three mutant structures. The local structure around the mutation site in F35Y is not obviously altered since F35 points toward the heme plane in the WT-Tb_5 and there is sufficient space to accommodate the additional hydroxyl group of Y35. The hydroxyl group is very close to the heme group, pointing toward a carbon atom of the heme, with the closest distance of 0.32 nm^2[13] indicating that Y35 makes very strong van der Walls contacts with the heme group, which leads to a slight decrease of the solvent accessibility of the heme-binding pocket. Table 1 shows that the solvent accessible area of its "pocket interior" decreases by 0.07 nm^2 compared with WT-Tb_5. This mutant is even more stable than WT-Tb_5, as shown in Table 1, which is unusual since for most of the proteins in nature various mutants are usually less stable than the wild type ones. The high stability of F35Y can be attributed to the strong van der Waals interactions of the hydroxyl group of Y35 with the heme group, which prevent the heme from leaving, and the slight increase of the hydrophobicity is also helpful for the stability.

Influence of the hydrophobicity of the heme-binding pocket on the redox potential

The redox potential is the driving force of the electron transfer between two redox proteins. The increase of the solvent accessible area of the "pocket interior" of each of P40V, V45E and V45Y compared with WT-Tb_5 is in the range of 0.26—0.49 nm^2, as shown in Table 1. The introduction of the negatively charged, electronegative or less hydrophobic groups to the edge of the heme-binding pocket makes the redox potential of each of the three mu-

tants shift negatively, in the range of 23—40 mV.

In the case of F35Y the slight increase of the hydrophobicity of the heme-binding pocket would not obviously influence the redox potential. However, the hydroxyl group of Y35 is located near the center instead of at the edge of heme-binding pocket, and this unusual location of the electronegative group leads to an exceedingly large shift of the redox potential in the negative direction (−66 mV).

References

1 Dreyer, J. L. *Experientia* **1984**, *40*, 653.
2 Mathews, F. S. *Prog. Biophys. Mol. Biol.* **1985**, *45*, 1.
3 Spatz, L.; Sttrittmatter, P. *Proc. Natl. Acad. Sci. U.S.A* **1971**, *68*, 1042.
4 Mathews, F. S.; Levine, M.; Argos, P. *J. Mol. Biol.* **1972**, *64*, 449.
5 Mathews, F. S.; Argos, P.; Levine, M. *Cold Spring Harber Quant Biol.* **1971**, *36*, 387.
6 Durley, R. C. E.; Mathews, F. S. *Acta Crystallogr.* **1996**, *D52*, 65.
7 Wu, J.; Gan, J. H.; Xia, Z. X.; Wang, Y. H.; Wang, W. H.; Xue, L. L.; Xie, Y.; Huang, Z. X. *Proteins: Struct. Funct. Genet.* **2000**, *40*, 249.
8 Rodgers, K. K.; Pochapsky, T. C.; Sliger, S. G. *Science* **1988**, *240*, 1657.
9 Rodgers, K. K.; Sliger, S. G. *J. Mol. Biol.* **1991**, *221*, 1453.
10 Rivera, M.; Seetharaman, R.; Girdhar, D.; Wirtz, M.; Zhang, X.; Wang, X.; White, S. *Biochemistry* **1998**, *37*, 1485.
11 Funk, W. D.; Lo, T. P.; Mauk, M. R.; Brayer, G. D.; MacGillivray, R. T. A.; Mauk, A. G. *Biochemistry* **1990**, *29*, 5500.
12 Sarma, S.; DiGate, R. J.; Goodin, D. B.; Miller, C. J.; Guiles, R. D. *Biochemistry* **1997**, *36*, 5658.
13 Yao, P.; Wu, J.; Wang, Y.-H.; Sun, B.-Y.; Xia, Z.-X.; Huang, Z.-X. *Eur. J. Biochem.* **2002**, *269*, 4287.
14 Wang, Z.-Q.; Wu, J.; Wang, Y.-H.; Qian, W.; Xie, Y.; Xia, Z.-X.; Huang, Z.-X. *Chin. J. Chem.* **2002**, *20*, 1212.
15 Gan, J.-H.; Wu, J.; Wang, Z.-Q.; Wang, Y.-H.; Huang, Z.-X.; Xia, Z.-X. *Acta Crystallogr.* **2002**, *D58*, 1298.
16 Xue, L.-L.; Wang, Y.-H.; Xie, Y.; Yao, P.; Wang, W.-H.; Qian, W.; Huang, Z.-X.; Wu, J.; Xia, Z.-X. *Biochemistry* **1999**, *38*, 11961.
17 Wu, J.; Wang, Y.-H.; Gan, J.-H.; Wang, W.-H.; Sun, B.-Y.; Huang, Z.-X.; Xia, Z.-X. *Chin. J. Chem.* **2002**, *20*, 1225.
18 Wang, Z.-Q.; Wang, Y. -H.; Wang, W.-H.; Xue, L.-L.; Wu, X.-Z.; Xie Y.; Huang, Z.-X. *Biophs. Chem.* **2000**, *83*, 3.
19 Yao, P.; Wang, Y.-H.; Sun, Y.-L.; Huang, Z.-X.; Xie, Y.; Xiao, G.-T. *Protein Eng.* **1998**, *10*, 578.
20 Lee, B.; Richards, F. M. *J. Mol. Biol.* **1971**, *55*, 379.
21 Collaborative Computational Project, Number 4. *Acta Crystallogr.* **1994**, *D50*, 760.
22 Evans, S. V. *J. Mol. Graphics.* **1993**, *11*, 134.
23 Roussel, A.; Cambillau, C. TURBO-FRODO, *Silicon Graphics Partner Geometry Dictionary*, edited by Silicon Graphics Inc, **1991**.

(E0304101 ZHAO, X. J.; DONG, L. J.)